Electronic Supplementary Material (ESI) for Energy & Environmental Science.

Electronic Supplementary Information

A modular strategy for decorating isolated cobalt atoms into multichannel carbon matrix for electrocatalytic oxygen reduction

Huabin Zhang,[a] Wei Zhou,[b] Tao Chen,[c] Bu Yuan Guan,[a] Zhen Li,[a] and Xiong Wen (David) Lou[a]*

[a] School of Chemical and Biomedical Engineering, Nanyang Technological University,62 Nanyang Drive, Singapore, 637459, Singapore.

E-mail: xwlou@ntu.edu.sg; davidlou88@gmail.com

Web: http://www.ntu.edu.sg/home/xwlou/

[b] Department of Applied Physics, Tianjin Key Laboratory of Low Dimensional Materials Physics and Preparing Technology, Faculty of Science, Tianjin University, Tianjin 300072, China.

[c] Beijing Synchrotron Radiation Facility (BSRF), Institute of High Energy Physics, Chinese Academy of Sciences, Beijing 100049, China.

Experimental details

Synthesis of cobalt porphyrins. Typically, cobalt nitrate (70 mg) was dissolved into ethanol solution (10 mL) by stirring at room temperature for 10 min. And then, the ligand of tetraphenyl porphyrin (TPP, 120 mg) was then added to this solution under stirring for 15 min. The mixture was then heated at 75 °C for 48 h. The microcrystalline powder was collected by evaporation and washed with water for three times.

Synthesis of PS-PAN and Co@PS-PAN nanowires. PS-PAN nanofibers were prepared by a previously reported method.[1] The precursor solution for electrospinning was prepared by dissolving PS (300 mg) and PAN (300 mg) in N, N-dimethylformamide (10 mL) with vigorous stirring at 60 ^{o}C overnight. Then PAN/PS composite nanofibers were electrospun on aluminum foil collector from the precursor solution. The distance between the syringe and the collector was fixed at 15 cm, and the voltage of 15 kV was applied with a flow rate of 1mL h^{-1}. The Co@PS-PAN nanofibers were synthesized by a similar method as PS-PAN except that additional 10 mg of cobalt porphyrins was added to the precursor solution.

Synthesis of MCM and Co@MCM. The MCM was obtained by pyrolyzing the PS-PAN nanofibers at 800 ^{o}C for 2 h with a heating rate of 3 ^{o}C min^{-1} under nitrogen atmosphere. Co@MCM was obtained by a similar method as MCM except that PS-PAN was replaced by Co@PS-PAN.

Materials characterizations. TEM and HRTEM were conducted on a Tecnai G2 F30 S-Twin electron microscope operated at 300 kV. Energy-dispersive X-ray (EDX) mappings were taken on a JEOL 2100F microscope. SEM images were recorded on a Hitachi S4800 microscope. Powder XRD was performed on an X'Pert PRO diffractometer with Cu Ka radiation (PANalytical). TG (Shimadzu DRG-60) was applied to trace the weight loss in the carbonization stage. Nitrogen adsorption-desorption isotherms were obtained by using a BELSORP-mini (Microtrac BELCorp.) at 77 K. ICP-MS was performed on a Thermo IRIS Intrepid II XSP spectrometer. Before measurement, the samples were degassed in a vacuum at 120 °C for 12 h. Surface chemical analysis was performed by XPS (PHI Quantera SXM, ULVAC-PHI Inc.).

X-ray absorption data collection, analysis, and modelling. Co K-edge X-ray absorption spectra were acquired at beamline 1W1B of the Beijing Synchrotron Radiation Facility (BSRF) in fluorescence mode at room temperature using a Si (111) double-crystal monochromator. The storage ring of BSRF was operated at 2.5 GeV with a maximum current of 250 mA in decay mode. The energy was calibrated using Co foil; the intensities of the incident and fluorescence X-ray were monitored by using standard N_2-filled ion chamber and Ar-filled Lytle-type detector, respectively. To achieve the best signal-to-noise ratio, the powdered samples were uniformly mixed with boron nitride powder and pressed to form a pellet, which was sealed in a cell holder with Kapton windows for XAFS measurement. A detuning of about 20% by misaligning the silicon crystals was also performed to suppress the high harmonic content.

The XAFS raw data were background-subtracted, normalized, and Fourier transformed by the standard procedures with the ATHENA program.[2] Least-squares curve fitting analysis of the EXAFS $\chi(k)$ data was carried out using the ARTEMIS program, with the theoretical scattering amplitudes, phase shifts and the photoelectron mean free path for all paths calculated by ab-initio code FEFF9.[3] All fits were performed in the *R* space with *k*-weight of 3. Due to the important non-MT effects in asymmetrical or sparse systems, the Co K-edge theoretical XANES calculations were carried out with the FDMNES code in the framework of full-potential finite difference method (FDM).[4] The energy dependent exchange-correlation potential was calculated in the real Hedin-Lundqvist scheme, and then the spectra are convoluted using a Lorentzian function with an energy-dependent width to account for the broadening due to both the core-hole width and the final state width.

Electrochemical Measurements. Linear sweep voltammetry (LSV) and chronoamperometry for oxygen reduction reaction (ORR) are conducted on a CHI 660D electrochemical workstation with a conventional three-electrode cell. Platinum and Ag/AgCl (3M KCl) electrodes are used as the counter electrode and reference electrode, respectively. The working electrode is prepared as follows: 3 mg catalyst is dispersed in the mixture of ethanol (0.6 mL) and Nafion (5 wt%, 30 μL) under ultrasonication for 30 min. Then, 20 μL of the above suspension is dropped on the polished glassy carbon electrode (5 mm in diameter) and dried at room temperature. The electrochemical measurements are performed in basic solution (0.1 M KOH) saturated with O_2 with a scan rate of 10 mV s^{-1}. The LSV curves for ORR are obtained by the rotating disk electrode (RDE) measurement.

Computational methods. All calculations were performed using Vienna ab initio package based on the DFT. The generalized gradient approximation was used for the exchange-correlation energy. In addition, the D2 method proposed by Grimme was adopted to describe the van der Waals interactions. A plane-wave expansion for the basis set with a cutoff energy of 400 eV was used. A vacuum region of 20 Å was used to eliminate interactions between the neighboring cells of slab models. Monkhorst k-point meshes (2 × 2 × 1) were used for the Brillouin-zone integrations of slab models with and without Co doping, respectively. All atoms were relaxed until the residual force was less than 0.01 eV/Å.

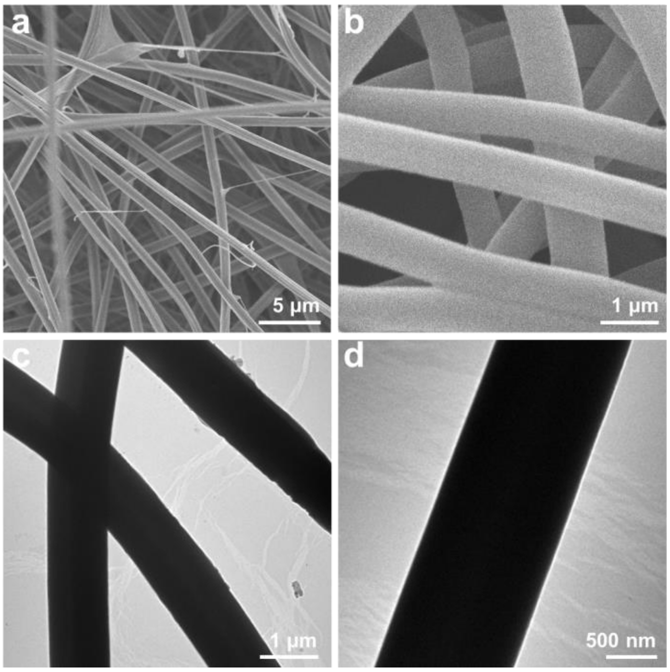

Fig. S1 (a, b) FESEM and (c, d) TEM images of Co@PS-PAN nanofibers.

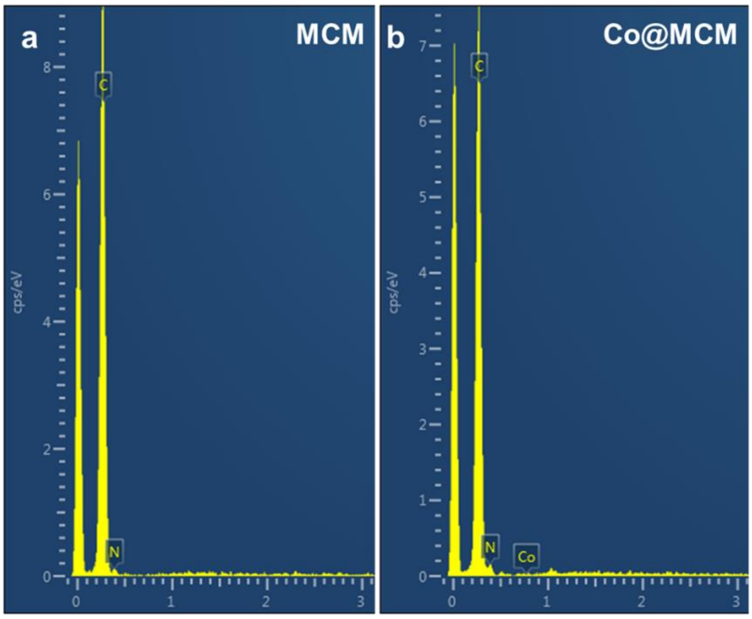

Fig. S2 EDX spectra of MCM (a) and Co@MCM (b).

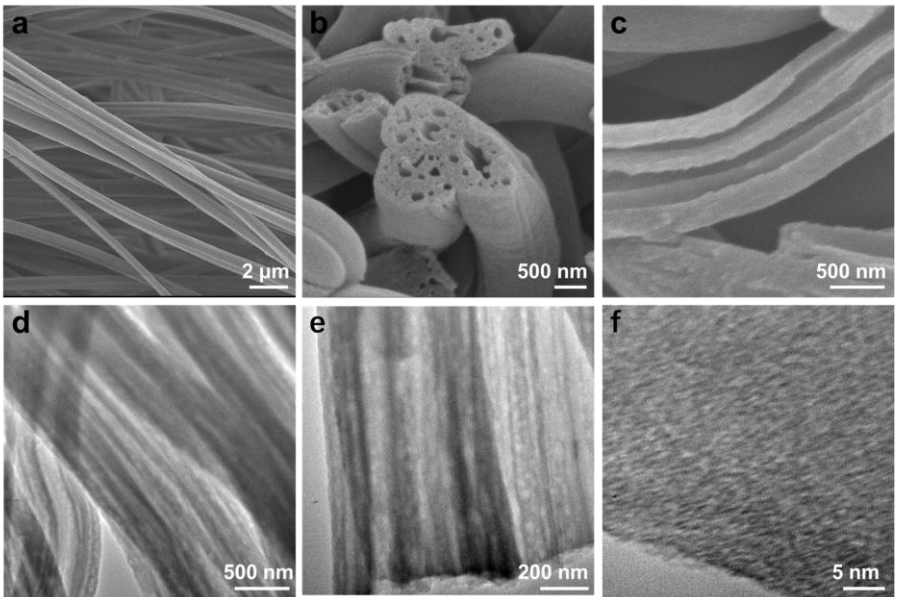

Fig. S3 (a-c) FESEM and (d-f) TEM images of MCM.

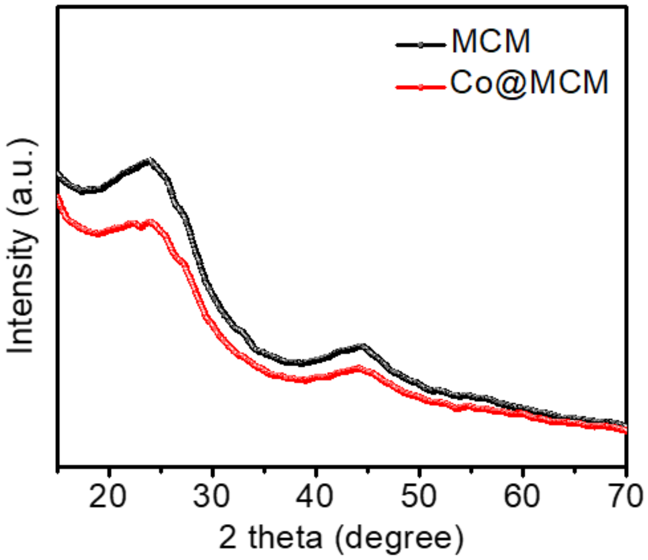

Fig. S4 XRD patterns of MCM and Co@MCM.

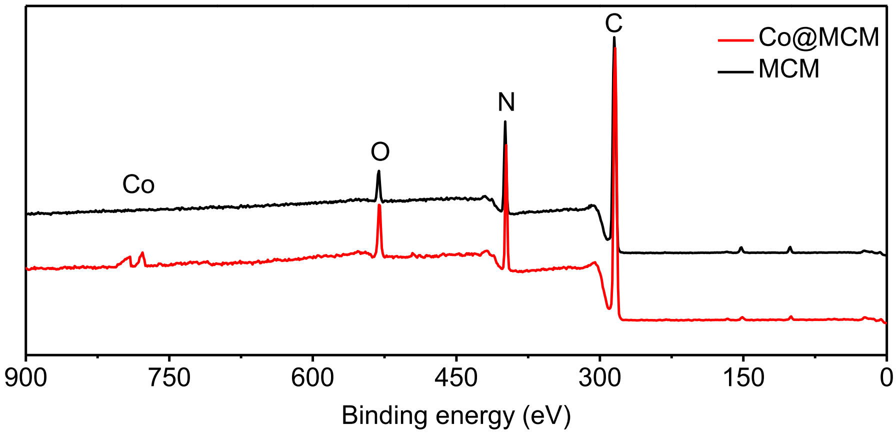

Fig. S5 Survey XPS spectra of Co@MCM and MCM.

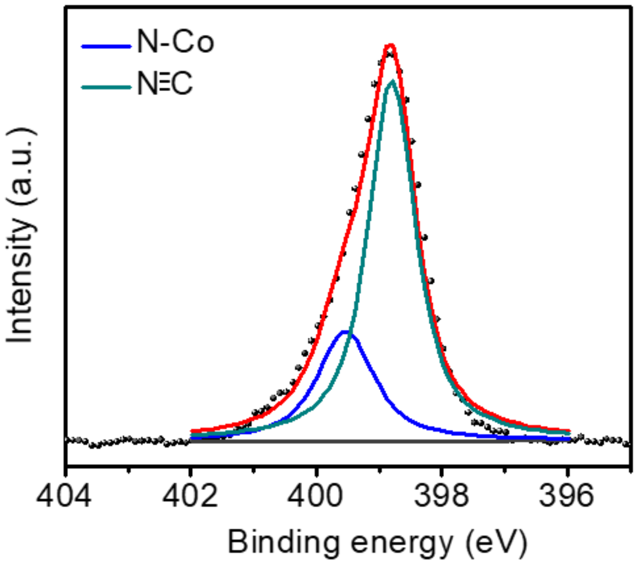

Fig. S6 N 1s spectrum of Co@PS-PAN.

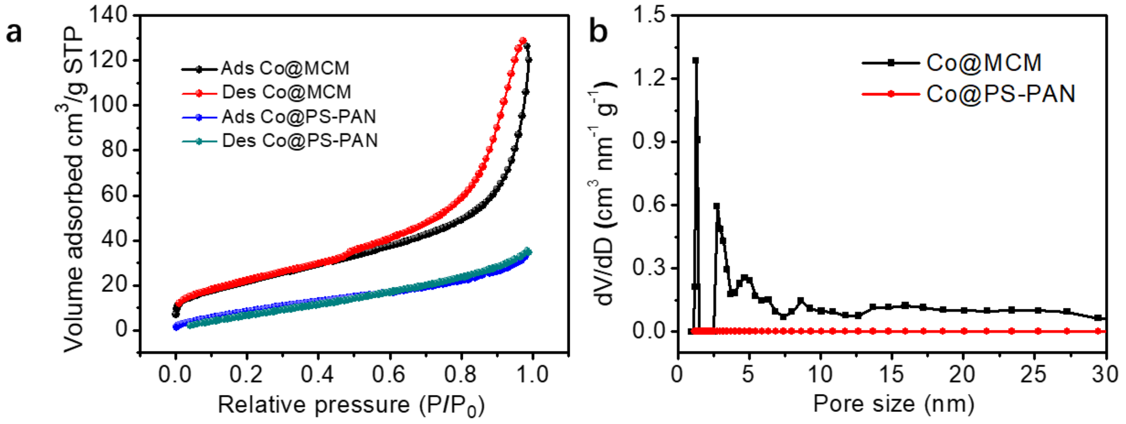

Fig. S7 (a) N_2 adsorption-desorption isotherms of Co@MCM and Co@PS-PAN. (b) Pore size distribution curves of Co@MCM and Co@PS-PAN.

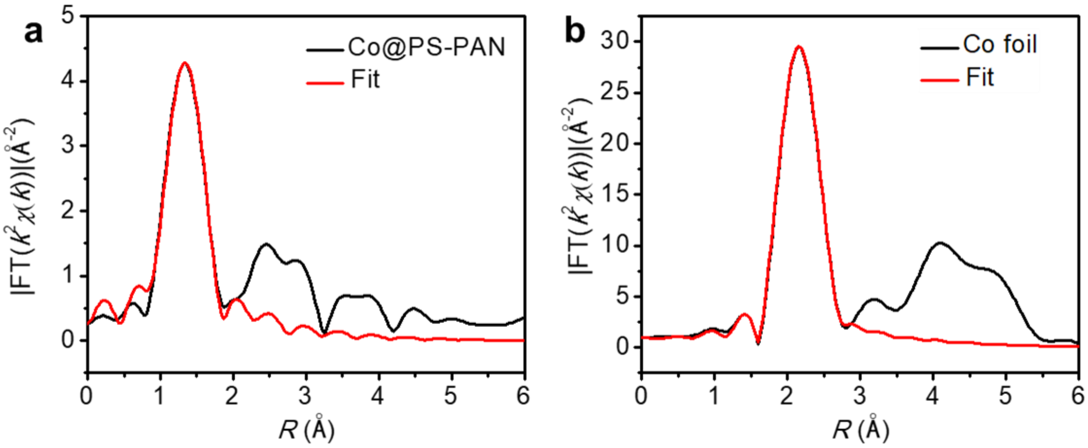

Fig. S8 Fourier transform of experimental EXAFS spectra and best fit results for Co@PS-PAN (a) and Co foil (b).

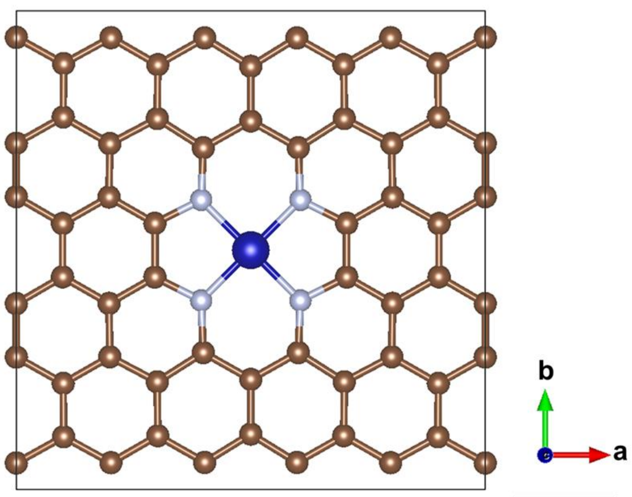

Fig. S9 Constructed model for an isolated cobalt atom, viewed from the *c* direction.

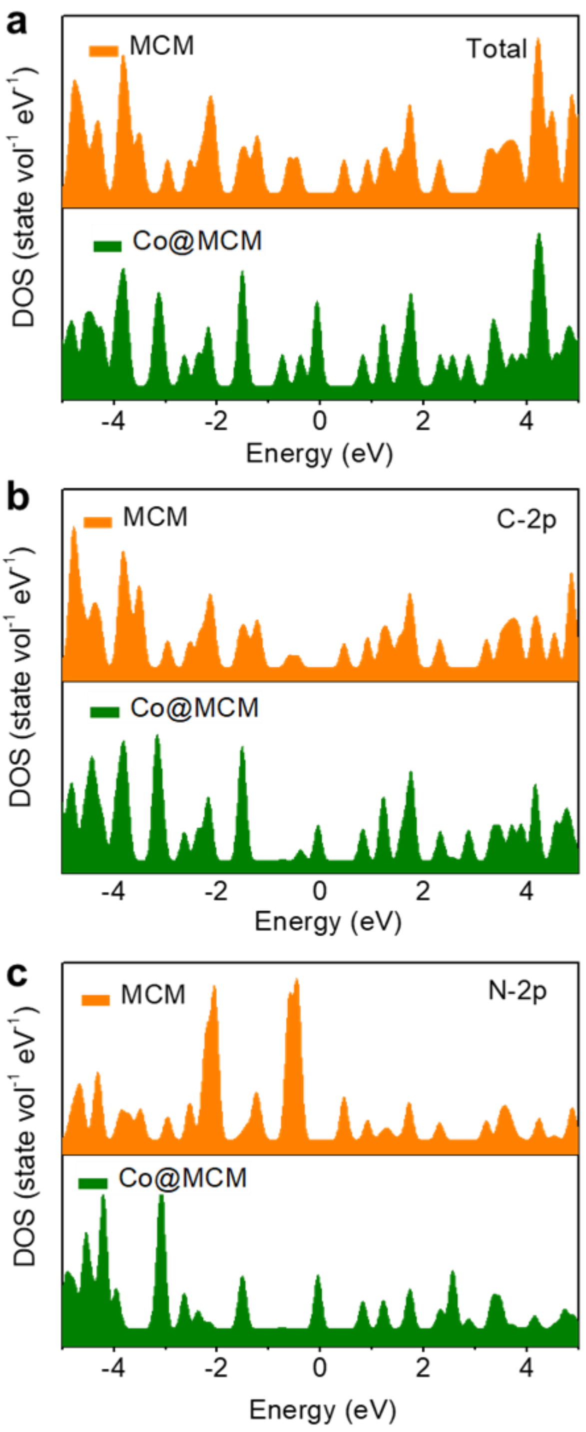

Fig. S10 Calculated DOS for total (a), C-2P (b) and N-2P (c) of MCM and Co@MCM.

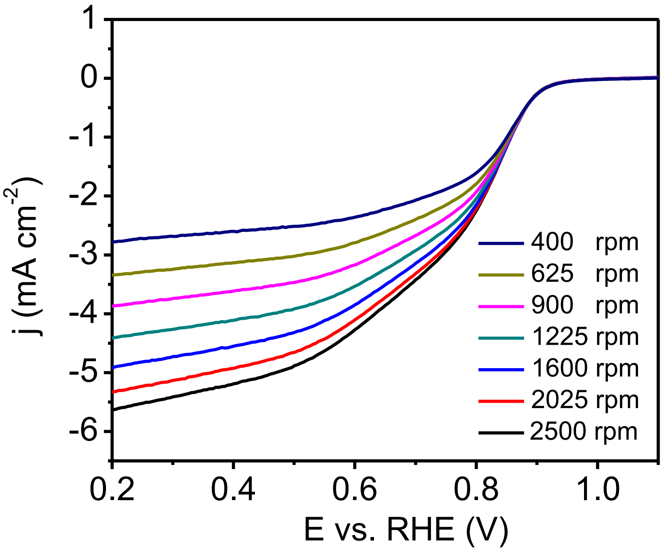

Fig. S11 LSV curves of Co@MCM-0.84% at different rotating rates in O_2-saturated 0.1 M KOH solution.

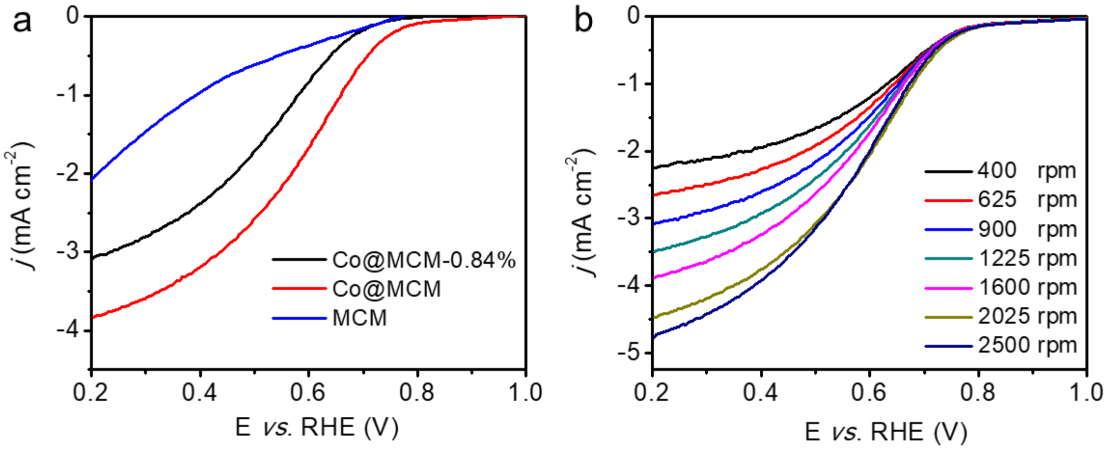

Fig. S12 (a) LSV curves of MCM and Co@MCM in O_2-saturated 0.5 M H_2SO_4 solution. (b) LSV curves of Co@MCM at different rotating rates in O_2-saturated 0.5 M H_2SO_4 solution.

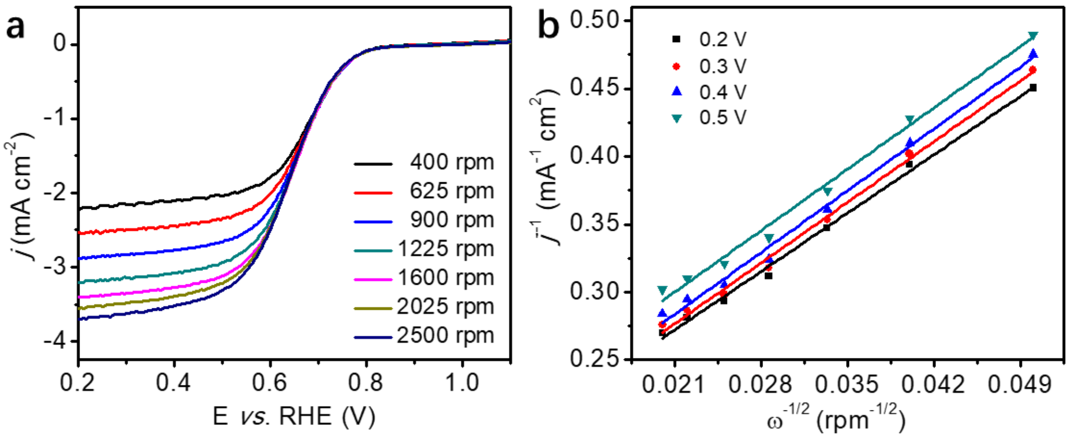

Fig. S13 (a) ORR polarization curves of MCM at different rotating rates in O_2-saturated 0.1 M KOH solution. (b) K-L plots for MCM.

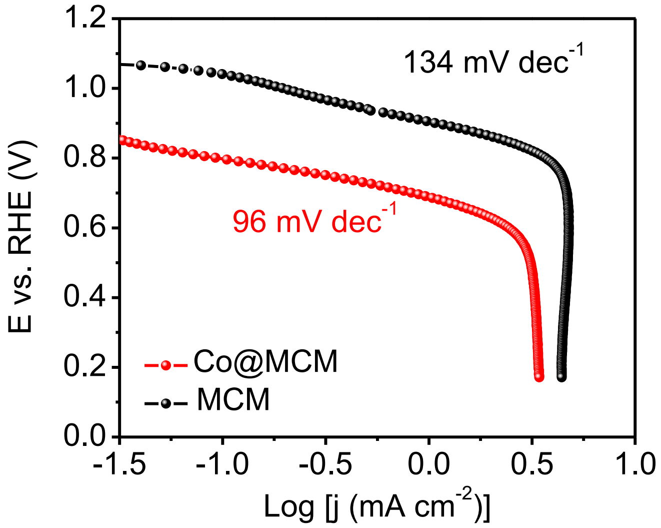

Fig. S14 Tafel plots of MCM and Co@MCM in O_2-saturated 0.1 M KOH solution.

.

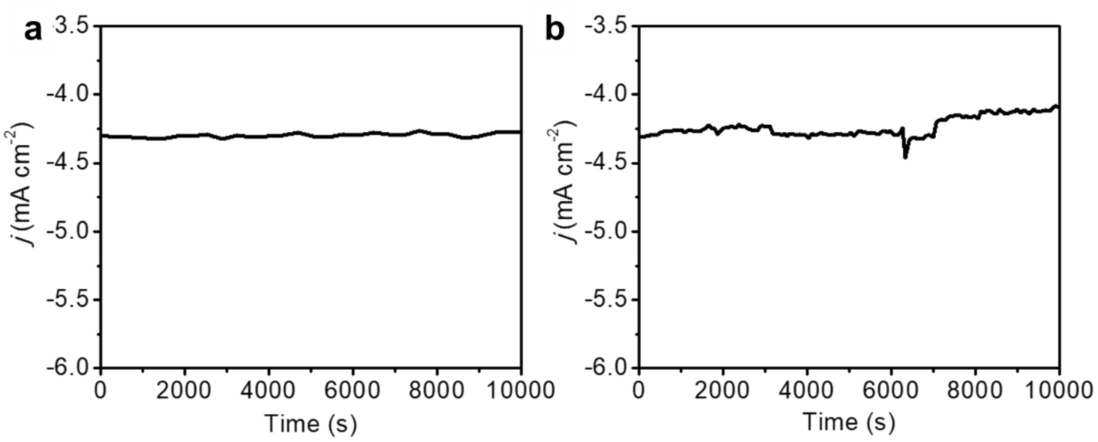

Fig. S15 (a) Durability test in O_2-saturated 0.1 M KOH at 0.5 V for Co@MCM. (b) Chronoamperometric response for Co@MCM, obtained at 0.5 V in O_2-saturated 0.1 M KOH solution (150 mL) with the addition of 10 mL of methanol at the time of 6500 s.

Table S1. Co K-edge EXAFS curve fitting parameters.

Sample	**Shell**	***N*** [a]	**EXAFS (Å)**	**σ^2 ($\times10^{-3}$ Å^{-2})** [b]	**ΔE_0** [c] **(eV)**	**R_f** [d]
Co foil [e]	Co-Co	12	2.50	7.1	6.18	0.001
Co@PS-PAN [f]	Co-N	4.14	2.01	9.15	-0.15	0.002
Co@MCM [g]	Co-N	2.21	1.90	2.54	-2.95	0.021
Co@MCM	Co-N	1.78	2.10	2.54	-2.95	0.021

[a] *N*, coordination number; [b] σ^2, Debye–Waller factor to account for both thermal and structural disorders; [c] ΔE_0 inner potential correction; [d] R_f factor (%) indicates the goodness of the fit. [e] Fitting range: 3.2 ≤ k (/Å) ≤ 12.5 and 1.4 ≤ R (Å) ≤ 2.7. [f] Fitting range: 2.0 ≤ k (/Å) ≤ 12.5 and 1.0 ≤ R (Å) ≤ 2.7. [g] Fitting range: 2.0 ≤ k (/Å) ≤ 12.5 and 1.0 ≤ R (Å) ≤ 2.0.

Table S2. Electrocatalytic performance of different Co/carbon-based electrocatalysts.

Catalyst	**Onset potential (V vs. RHE)**	**Half-wave potential (V vs. RHE)**	**CV peak potential (V *vs.* RHE)**	**Limiting current density (mA cm^{-2})**	**Ref.**
CNT/PC	0.85	0.76	N/A	5.8	5
Co/graphene sheets	0.80	0.75	N/A	3.7	6
CNCo	0.89	0.82	0.81	5.3	7
N-doped hollow fibers	0.87	0.80	0.78	5.6	8
Graphene/Co_3O_4 sheets	0.95	N/A	N/A	3.9	9
N-GS	0.91	0.83	N/A	3.2	10
Ordered mesoporous carbon	0.81	0.69	N/A	3.1	11
Co@MCM	0.95	0.78	0.77	4.9	This work

Supplementary References

1. Z. Li, J. T. Zhang, Y. M. Chen, J. Li and X. W. D. Lou, *Nat. Commun.*, 2015, **6**, 8850.
2. B. Ravel and M. Newville, *J. Synchrotron Radiat.*, 2005, **12**, 537.
3. J. J. Rehr and R. C. Albers, *Rev. Mod. Phys*, 2000, **72**, 621.
4. Y. Joly, *Phys. Rev. B*, 2001, **63**, 125120.
5. Y. J. Sa, D.-J. Seo, J. Woo, J. T. Lim, J. Y. Cheon, S. Y. Yang, J. M. Lee, D. Kang, T. J. Shin and H. S. Shin, *J. Am. Chem. Soc.*, 2016, **138**, 15046-15056.
6. G. Wu, K. L. More, C. M. Johnston and P. Zelenay, *Science*, 2011, **332**, 443-447.
7. Y. Z. Chen, C. Wang, Z. Y. Wu, Y. Xiong, Q. Xu, S. H. Yu and H. L. Jiang, *Adv. Mater.*, 2015, **27**, 5010-5016.
8. W. Zhang, Z.-Y. Wu, H.-L. Jiang and S.-H. Yu, *J. Am. Chem. Soc.*, 2014, **136**, 14385-14388.
9. S. Li, D. Wu, C. Cheng, J. Wang, F. Zhang, Y. Su and X. Feng, *Angew. Chem., Int. Ed.*, 2013, **52**, 12105-12109.
10. H. B. Yang, J. Miao, S.-F. Hung, J. Chen, H. B. Tao, X. Wang, L. Zhang, R. Chen, J. Gao and H. M. Chen, *Sci. Adv.*, 2016, **2**, e1501122.
11. S. Lee, M. Choun, Y. Ye, J. Lee, Y. Mun, E. Kang, J. Hwang, Y. H. Lee, C. H. Shin and S. H. Moon, *Angew. Chem., Int. Ed.*, 2015, **54**, 9230-9234.